Land Movement Detection from UAV Images for a Sustainable World

Pamela C. Pesántez-Cabrera [1]*

[1] Universidad Católica de Cuenca, School of Civil Engineering, Cuenca – Ecuador; (pamela.pesantez)@est.ucacue.edu.ec

Commission II/WG 2

Keywords: Photogrammetry, Land movement, UAV images, Landslide, Sustainable.

Abstract

In Reina del Cisne (Cuenca-Ecuador), a dynamic sliding process occurred due to a cut made at the beginning of 2018 on the hillside without technical considerations for the construction of an access road to a house in the sector. From January 2019 to June 2019, the period analyzed in this work, the landslide caused complete structural damage to dwellings near the hillside and partial damage to houses farther away. It also led to the total collapse of the path that initiated the landslide. Field visits and comparisons using CloudCompare of point clouds obtained from UAV flights between January 2019 and June 2019 highlighted the high activity of this landslide. The analysis demonstrates the effectiveness of this technique for early detection of landslides, enabling timely warnings for inhabitants to take immediate measures to avoid disasters.

1. INTRODUCTION

Landslides are among the most destructive geological processes affecting humans, causing deaths and property losses worth tens of trillions of dollars each year (Brabb & Harrod, 1989). In Cuenca-Ecuador, many inhabitants build their homes on steep slopes due to the low prices of such lands and the rapid urban growth. These slopes often experience landslides, which damage constructions, as seen in the Reina del Cisne sector. It is essential to monitor these slides for accurate mapping, urban planning, and risk prevention. Monitoring can be done using classical in-situ topographic techniques such as differential GNSS or total station (González-Zúñiga, 2010), combined with active sensors like RADAR (Bardi et al., 2014; Martire et al., 2016; Ventisette et al., 2014), UAVs (Dewitte et al., 2008; Martínez-Espejo Zaragoza et al., 2017; Buffi et al., 2017), or satellite images (Behling & Roessner, 2017). Detecting large landslides is challenging, requiring significant economic and human resources and long periods, typically weeks or months. Changing climatic conditions, such as heavy rains, also cause morphological variations. In Ecuador, heavy rains often lead to landslides, necessitating improved detection processes for at-risk areas. This study aims to monitor and record sliding movements on a steep hillside in the Reina del Cisne sector (SE Cuenca) affecting several homes, providing recommendations and future work directions.

2. METHODS

The study area was delimited using PPGIS (Public Participation Geographic Information System). Figure 1 shows the study area located at UTM coordinates 17 S area, 726.775 m E and 9.679.327 m N, with an elevation of 2600 m, characterized by steep slopes.
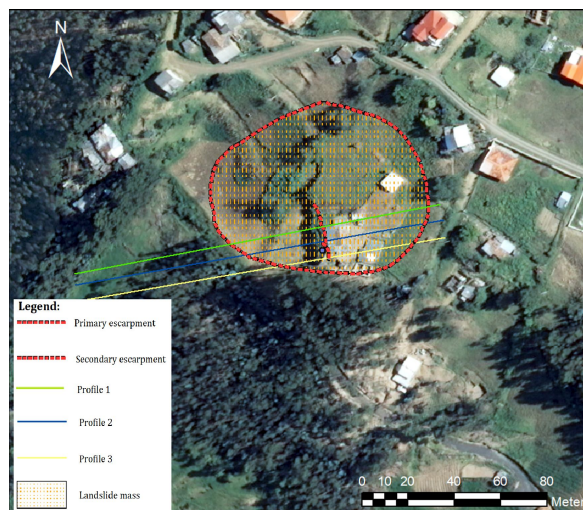

Figure 1. Study area (Cuenca – Ecuador) with information about the landslide and distribution of the profiles studied

2.1 Generation of point clouds using UAV

The UAV used was a DJI Phantom 4 RTK®. This UAV is ideal for mapping, inspection, and surveying, featuring a high-resolution camera capable of capturing RTK data with centimeter-level accuracy and requiring fewer ground control points compared to traditional tools (Peppa et al., 2019). The UAV can produce orthomosaics, point clouds, and digital elevation models (DEM) with a precision of 3 cm (Mulakala, 2019).

The flight was configured using the Pix4capture© mobile application in double grid flight mode for 3D models (Figure 2).

* Corresponding author

Details	Description
Flight altitude	50 m
Images per flight	219
Flight area	312 x 216 m
Flight time	29 minutes
Ground sample distance	1.45 cm/px

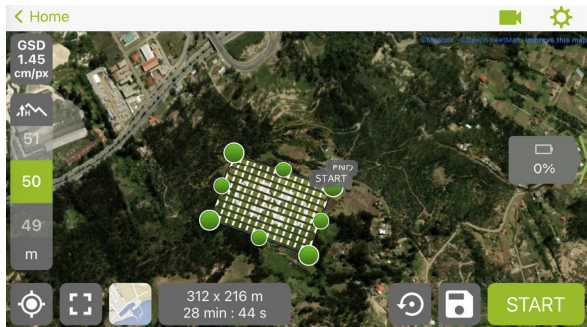**Table 1**. Details for January 2019 and June 2019 flights

Figure 2. Flight configuration in the Pix4capture© application

The two sets of images from January 2019 and June 2019 were processed using Agisoft PhotoScan© software. The processing steps included: 1) photograph selection; 2) camera calibration; 3) finding homologous points; and 4) identifying points over the terrain. The UAV made real-time corrections and triangulations to adjust the images, generating point clouds, orthophotos, and DEM (Núñez Calleja, 2016).

After processing, two point clouds were obtained with densities shown in Table 2.

Date	Points
January 2019	78 million
June 2019	75 million

Table 2. Point clouds density

2.1.1   Errors obtained in the point clouds generation: The joining of scans to form each of the 2 points clouds was satisfactory. The highest average error for the two dates was only 2.3 cm (Figure 3).

Points	Error (cm)
P1	0.4
P2	2.4
P3	2.7
P4	5.8
P5	2.6
P6	5.2
P7	3.9
Average	2.3

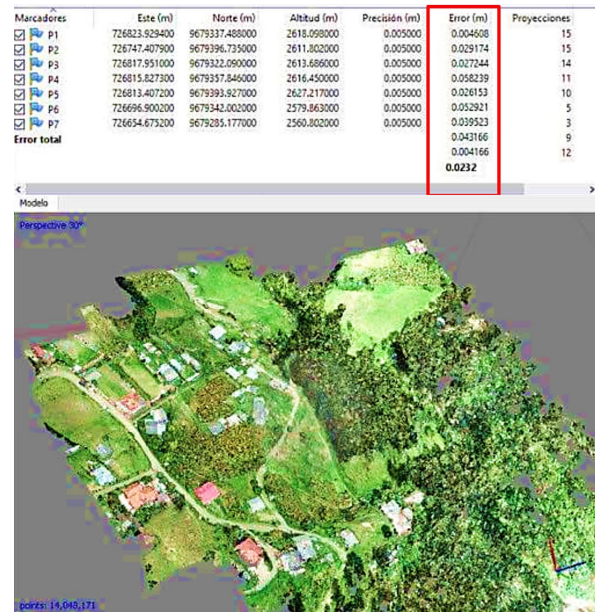**Table 3**. Error values in the point clouds generation

Figure 3. Average errors in m the generation of points clouds

2.2   CloudCompare

To align and compare in CloudCompare the point clouds of both dates (January 2019 and June 2019) were used 12 static reference points, located outside the landslide area indicated in Figure 4. In addition, a comparison has been made of the deformations that the dwelling has suffered using the same 12 reference points located outside the main escarpment (January 2019 and June 2019).

2.2.1   Errors obtained in the point clouds alignment: The 12 reference points were precisely located and selected in each of the point clouds to align them. The points (A) correspond to the January point cloud and the points (R) correspond to the June point cloud, for the first alignment, which is indicated in Figure 4.

The alignment errors were minimal, with all errors below 1 mm, as shown in Table 4.

Points	Error (mm)
A0 – R0	0.3
A1 – R1	0.2
A2 – R2	0.3
A3 – R3	0.2
A4 – R4	0.3
A5 – R5	0.2
A6 – R6	0.5
A7 – R7	0.3
A8 – R8	0.4
A9 – R9	0.2
A10 – R10	0.3
A11 – R11	0.3

Table 4. Error values in the alignment between January 2019 and June 2019 clouds
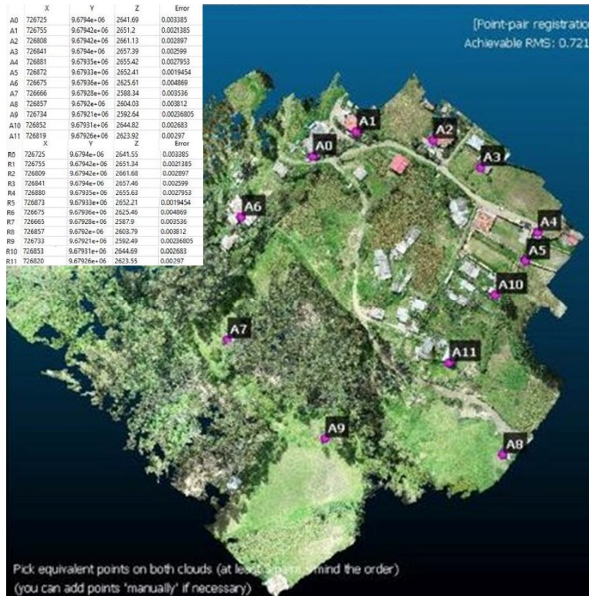
Figure 4. Location of point cloud alignment points with their error values

2.2.2   Profiling in aligned point clouds: After aligning the point clouds (January 2019 and June 2019), three profiles were extracted for each point cloud (six in total) as shown in Figure 1. The profiles were obtained using CloudCompare's extract cloud section tool and saved as LAS files for use in AutoCAD® Civil 3D.

Figure 5. Profile extraction process

2.3   AutoCAD ® Civil 3D

The profiles obtained in CloudCompare were exported to represent, locate, and quantify the movements caused by the landslide (Figures 6, 8, and 10).
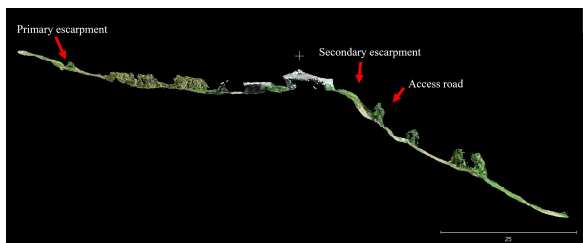

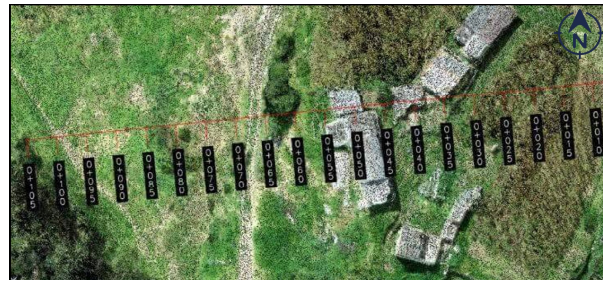**Figure 6.** Profile 1 exported to AutoCAD® Civil 3D – Side view

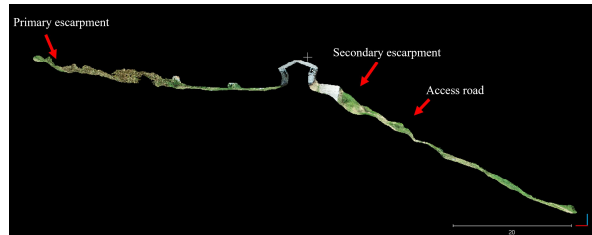**Figure 7.** Profile 1 exported to AutoCAD® Civil 3D – Top view

Figure 8. Profile 2 exported to AutoCAD® Civil 3D – Side view

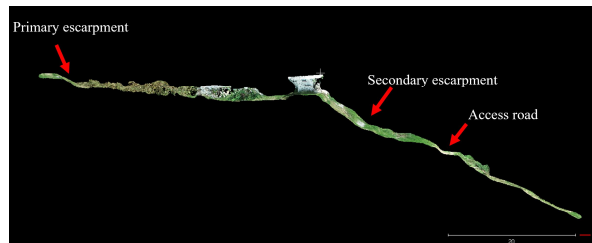**Figure 9.** Profile 2 exported to AutoCAD® Civil 3D – Top view

Figure 10. Profile 3 exported to AutoCAD® Civil 3D – Side view
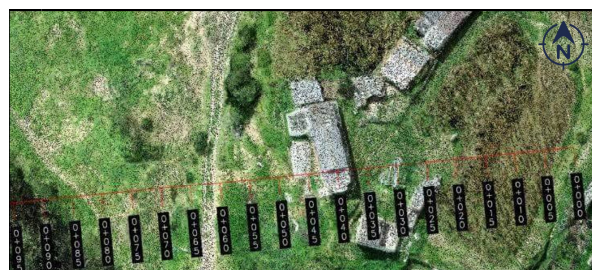

Figure 11. Profile 3 exported to AutoCAD® Civil 3D – Top view

3. DETECTION OF LANDSLIDE ACTIVITY BASED ON THE EXTRACTED POINT CLOUDS

The segmentation method for scanning profiles was used for comparing profiles by segmenting the point cloud along lines. This technique involves freely drawing a profile across the points. The tracing of this line can be done where it is most convenient (Gonzalez et al., 2004), in this case, along the terrain where the landslide showed the most activity during field visits.The profile representation was generated using AutoCAD® Civil 3D with the extracted profiles from the point clouds (January 2019 and June 2019). This provided profiles with relevant landslide movement information.

3.1 Procedure with extracted profiles

The method for comparing profiles (January 2019 and June 2019) involved exporting the point clouds to AutoCAD® Civil 3D, creating a surface from the point cloud, drawing a line along the zone of interest at the top of the point cloud, creating a profile of the surface corresponding to the line, and extracting and displaying the abscissas and heights information for the profile. Figures 12, 13, and 14 show the three January 2019 point cloud profiles.
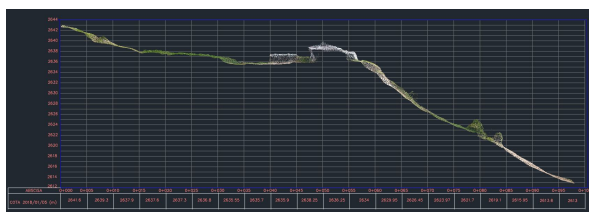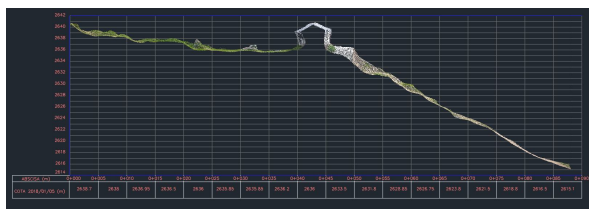

Figure 12. Profile 1 in AutoCAD® Civil 3D

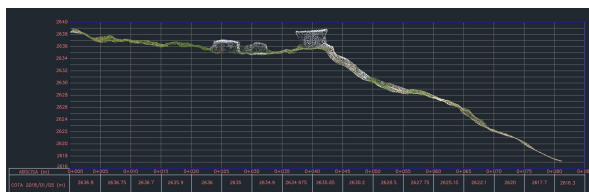**Figure 13.** Profile 2 in AutoCAD® Civil 3D

Figure 14. Profile 3 in AutoCAD® Civil 3D

4. RESULTS

The dimensions of each point cloud and their differences were correctly analyzed for profile comparison. A 5 m division was used for abscissas and a 2 m division for heights. Each profile was superimposed with both point clouds to illustrate and quantify the deformations in the study area during the analyzed period (January 2019 and June 2019).

4.1 Profiles comparison

In Profile 1, 2 and 3, (Figure 1, 15, 16 and 17), it is observed that the growth of corn (abscissa 0+015 to 0+035); in general, it is seen as the ground sinks (abscissa 0+040 to 0+073) and as slowly it is rising (abscissa 0+075 to 0+105).

In Profile 1, (Figure 15) and Profile 3, (Figure 17) are displayed along the same as the recorded terrain movements, although they are removed from the central axis of the landslide these are produced by mini-slides produced by secondary escarpments.

In Profile 2, (Figure 16), it can be noticed that the recorded movements are greater, this is because the profile is located in the central axis of the landslide, besides being influenced by the movements of the mini-landslide produced by a secondary escarpment.
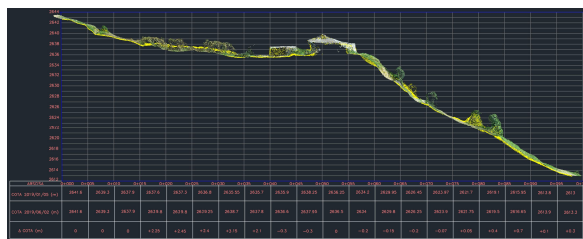

Figure 15. Comparison profile 1, January 2019 (yellow) and June 2019 (RGB).
+: Growth or uplift.
-: Sinking.

Figure 16. Comparison profile 2, January 2019 (yellow) and June 2019 (RGB).
+: Growth or uplift.
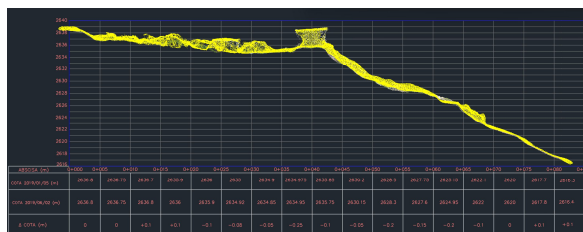-: Sinking.

Figure 17. Comparison profile 3, January 2019 (yellow) and June 2019 (RGB).
+: Growth or uplift.
-: Sinking.

5. CONCLUSIONS

This study successfully demonstrated the application of UAV photogrammetry and point cloud analysis to detect and monitor landslides in the Reina del Cisne sector of Cuenca, Ecuador. The main conclusions drawn from this research are as follows:

Effectiveness of UAV Photogrammetry:

The use of a DJI Phantom 4 RTK® UAV provided high-resolution imagery that facilitated the generation of accurate point clouds and digital elevation models (DEMs).

The UAV method proved to be efficient and cost-effective, reducing the need for extensive ground control points and providing rapid data acquisition suitable for landslide monitoring.

Point Cloud Comparison:

By comparing point clouds generated from UAV images taken in January 2019 and June 2019, significant land movements were detected. The high density of points (78 million in January and 75 million in June) ensured detailed analysis.

The alignment and profiling of these point clouds using CloudCompare and AutoCAD® Civil 3D allowed for precise quantification of deformations and provided valuable insights into the extent and progression of the landslide.

Landslide Activity Detection:

The study identified critical zones of movement and deformation on the hillside, indicating ongoing landslide activity. The profiles extracted showed notable displacements, which were crucial for understanding the dynamics of the landslide.

The methodology highlighted the potential for early warning systems, as regular UAV surveys can detect changes over time, allowing for timely interventions and risk mitigation.

Implications for Urban Planning and Safety:

The findings underscore the importance of integrating advanced monitoring techniques in urban planning, especially in areas prone to landslides. This can lead to better-informed decisions, safer construction practices, and enhanced disaster preparedness.

The study also emphasizes the need for continuous monitoring and the establishment of early warning systems to protect inhabitants and minimize property damage.

Future Work:

Future research should focus on extending the monitoring period and incorporating additional data points to improve the accuracy of predictions.

Integrating other remote sensing technologies, such as LiDAR and InSAR, could provide complementary data to enhance the understanding of landslide mechanisms.

There is also a need to develop automated systems for real-time data processing and analysis, facilitating quicker response times and more effective landslide management.

In conclusion, UAV photogrammetry combined with point cloud analysis presents a robust tool for landslide detection and monitoring, offering significant benefits for sustainable urban development and disaster risk reduction.

References

Barbarella, M., & Fiani, M., 2013. Monitoring of large landslides by Terrestrial Laser Scanning techniques: field data collection and processing. European Journal of remote sensing, 46(1), 126-151. doi.org/10.5721/EuJRS20134608.

Bardi, F., Frodella, W., Ciampalini, A., Bianchini, S., Ventisette, C. Del, Gigli, G., … Casagli, N., 2014. Integration between ground based and satellite SAR data in landslide mapping: The San Fratello case study. Geomorphology, 223, 45–60. doi.org/10.1016/j.geomorph.2014.06.025.

Behling, R., & Roessner, S., 2017. Spatiotemporal landslide mapper for large areas using optical satellite time series data. En Workshop on World Landslide Forum (pp. 143-152).

Brabb, E. E., & Harrod, B. L., 1989. Landslides: extent and economic significance. Proceedings of the 28th International Geological Congress: Symposium on Landslides.

Buffi, G., Manciola, P., Grassi, S., Barberini, M., & Gambi, A., 2017. Survey of the Ridracoli Dam: UAV–based photogrammetry and traditional topographic techniques in the inspection of vertical structures. Geomatics, natural hazards and risk, 8(2), 1562-1579. doi.org/10.1080/19475705.2017.1362039.

Eeckhaut, M. Van Den, Poesen, J., Gullentops, F., Vandekerckhove, L., & Hervás, J., 2011. Regional mapping and characterisation of old landslides in hilly regions using LiDAR-based imagery in Southern Flanders. Quaternary Research, 75(3), 721–733. doi.org/10.1016/j.yqres.2011.02.006.

González-Zúñiga, J. C., 2010. Monitorización de deslizamientos de ladera mediante estación total y GPS diferencial. Aplicación al deslizamiento del kilómetro 35+000 de la vía Loja-Cuenca (Ecuador), 71.

Gonzalez, R. C., Woods, R. E., & Eddins, S. L., 2004. Digital image processing using MATLAB. (Vol. 624). PearsonPrentice Hall Upper Saddle River.

Martínez-Espejo Zaragoza, I., Caroti, G., Piemonte, A., Riedel, B., Tengen, D., & Niemeier, W., 2017. Structure from motion (SfM) processing of UAV images and combination with terrestrial laser scanning, applied for a 3D-documentation in a hazardous situation. Geomatics, Natural Hazards and Risk, 8(2), 1492-1504. doi.org/10.1080/19475705.2017.1345796.

Martire, D. Di, Tessitore, S., Brancato, D., Ciminelli, M. G., Costabile, S., Costantini, M., … Calcaterra, D., 2016. Landslide detection integrated system (LaDIS) based on insitu and satellite SAR interferometry measurements. CATENA, 137, 406–421. doi.org/10.1016/j.catena.2015.10.002.

Mulakala, J., 2019. Measurement Accuracy of the DJI Phantom 4 RTK & Photogrammetry. DroneDeploy, Tech. Rep.

Núñez Calleja, P., 2016. Comparativa de software para la realización de ortofotos a partir de imágenes obtenidas por drones.

Peppa, M. V., Hall, J., Goodyear, J., & Mills, J. P., 2019. Photogrammetric assessment and comparison of DJI Phantom 4 pro and phantom 4 RTK small unmanned aircraft systems. ISPRS Geospatial Week 2019.

Revuelto, J., López-Moreno, J. I., Azorín-Molina, C., Arguedas, G., Vicente Serrano, S. M., & Serreta Oliván, A., 2013. Utilización de técnicas de láser escáner terrestre en la monitorización de procesos geomorfológicos dinámicos: el manto de nieve y heleros en áreas de montaña.

Štroner, M., Křemen, T., Braun, J., Urban, R., Blistan, P., & Kovanič, L., 2019. Comparison of 2.5 D Volume Calculation Methods and Software Solutions Using Point Clouds Scanned Before and After Mining. Acta Montanistica Slovaca, 24(4).

Travelletti, J., Malet, J.-P., & Delacourt, C., 2014. Image-based correlation of Laser Scanning point cloud time series for landslide monitoring. International Journal of Applied Earth Observation and Geoinformation, 32(0), 1–18. doi.org/10.1016/j.jag.2014.03.022.

Ventisette, C., Righini, G., Moretti, S., & Casagli, N., 2014. Multitemporal landslides inventory map updating using spaceborne SAR analysis. International Journal of Applied Earth Observation and Geoinformation, 30, 238– 246. doi.org/10.1016/j.jag.2014.02.008.